



## The Beauty of Mathematical Functions - Measurement of PVC Melt Viscosities by Torque Rheometer - Part I

Michael Schiller (HMS Concept e.U., Arnoldstein, Austria), Martin Schwarz (Brabender GmbH & Co. KG, Duisburg, Germany), Hitesh K. Singh (Platinum Industries Pvt. Ltd., Mumbai, India)

**Abstract:** The plasticorder also called laboratory kneader, batch mixer, plastograph, torque rheometer... can be considered as an “extruder” with extremely short screws. It imparts significant friction (torque) onto the dry blend in a short time. Normally the results of such experiment are depicted by a graph of torque vs. time resp. temperature vs. time. However, it can be also considered as a kind of viscosimeter. In this case, it is possible to simulate the rheometer graph by a mathematical function which allows to compare rheometer graphs at the same mass temperature. We also proved proof that it is possible to measure shear stress resp. viscosities by using a torque rheometer. We found an excellent correlation between calculated shear stress  $\tau/k$  (rheometer) and the viscosity  $\eta$  (single screw extruder).

Keywords: Polyvinyl chloride, PVC, Rheometer, Viscosimeter, Viscosity, Shear stress, Shear rate

### 1. Introduction

Various methods are used in the PVC industry to determine the processing behavior in the laboratory on different devices such as:

- Plastograph
- Single screw extruder
- Counter-rotating twin-screw extruder.

The results of one of these methods are rarely transferrable to another. However, they all have a right to exist.

Both the single screw extruder and the counter rotating twin-screw extruder will deliver information about:

- Extrusion torque
- Extrusion pressures and pressure buildup if several pressure sensors are available
- Melt temperature
- Melt viscosity if there is a pressure sensor both in the barrel at the end of the screw and in the die.

The plasticorder also called laboratory kneader, batch mixer, plastograph, torque rheometer or simply after the 1st brand called Brabender can be considered as an “extruder” with extremely short screws. It has an enclosed chamber, which allows measurements at different temperatures. The result of the measurements is influenced by the temperature, the kneader’s rotational speed, the filling volume and of course of the additives inside. This measuring device imparts significant friction (torque) onto the dry blend in a short time. Normally the results of a kneader experiment are depicted by a graph of torque vs. time resp. temperature vs. time. In principle it looks like that there isn’t any way to get any information about viscosity from the plasticorder in an easy way...

However, in 1967 Goodrich and Porter<sup>1</sup> reported that the Brabender torque rheometer qualitative indications of melt viscosity and viscosity-temperature dependence beside



other information which were not consider prior their paper. They wrote: „The following relations apply to a Newtonian liquid in rotational viscosimeters:

$$\tau = K_1 \cdot M \tag{1}$$

where  $\tau$  is the shear stress and  $M$  is the torque;

$$\gamma = K_2 \cdot S \tag{2}$$

where  $\gamma$  is the shear rate and  $S$  is the speed of rotation of the inner cylinder;

$$\eta = (\tau/\gamma) = (K_1 \cdot M)/(K_2 \cdot S) \tag{3}$$

where  $\eta$  is the viscosity. For Newtonian fluids,  $K_1$  and  $K_2$  are constants which depend only on the dimensions of the viscosimeter if all the variables are expressed in cgs units“; (cgs = Centimetre–gram–second system of units)

We can simplify Equation 3 to Equation 4 by replacing  $(K_1/K_2)$  by an equipment related constant  $k$ :

$$\eta = (k \cdot M/S) = (\tau/\gamma) \tag{4}$$

If we apply this to torque rheometer we will receive:

$$\eta \cdot \gamma = \tau = k \cdot M \tag{5}$$

and

$$M = (\eta \cdot \gamma)/k = \tau/k \tag{6}$$

The dependency of the viscosity  $\eta$  of a Newtonian fluid on temperature was firstly reported by Raman<sup>2</sup> and is today known as Andrade equation<sup>3</sup>; Equation 7:

$$\eta = \eta_0 \cdot e^{(E_a/R \cdot T)} \tag{7}$$

where is  $\eta_0$  the intrinsic viscosity,  $E_a$  is the flow activation energy,  $R$  is the universal gas constant, and  $T$  is the absolute temperature in Kelvin (K). However, PVC is not a Newtonian fluid. It is a pseudoplastic, a shear thinning fluid. Nevertheless, we can assume that PVC can considered in a small temperature range of e.g. 20 degree to behave Newtonian according to Equation 7. If we assume that Equation 4 can also be transferred to the intrinsic viscosity  $\eta_0$  in Equation 7 it will result in Equation 8:

$$\eta = (\tau/\gamma) = (\tau_0/\gamma) \cdot e^{(E_a/R \cdot T)} = k \cdot (M/S) = k \cdot (M_0/S) \cdot e^{(E_a/R \cdot T)} \tag{8}$$

where  $M_0$  is the intrinsic torque which is a linear function of the shear stress  $\tau_0$ . If we now multiply Equation 5 with the speed of rotation of the inner cylinder  $S$  and divide by the equipment related constant  $k$  it will result in Equation 9:

$$M = M_0 \cdot e^{(E_a/R \cdot T)} \tag{9}$$

This means more or that the torque  $M$  of the rheometer is a function of the shear stress  $\tau$ . In this case it will be possible to calculate the flow activation energy  $E_a$  and the intrinsic torque  $M_0$ . resp. the „shear stress“  $k \cdot \tau_0$ .



Finally, it shall be possible to find a correlation of  $M_0$  on torque rheometer with the viscosity  $\eta$  measured by extrusion on extruder with pressure sensors at the end of the screw(s) and in a slot or round capillary die. Following equations are applied to calculate the shear stress  $\tau$  and the shear rate  $\dot{\gamma}$  in the case of a slot die<sup>4</sup>:

$$\tau = (\Delta P \cdot H)/(2 \cdot L) \quad (10)$$

$$\dot{\gamma} = (6 \cdot V)/(W \cdot H^2) \quad (11)$$

wherein is:

- $\Delta P$ : the pressure difference (in Pa) between pressure transducers D2 and D3 in Figure 1
- H: the height of the slot capillary in cm
- L: the distance between the pressure transducers D2 and D3 (Figure 3) in the capillary of the slot capillary in cm
- V: the volumetric throughput in mL/s
- W: the width of the slot capillary in cm

The viscosity can be calculated by Equation 3.

A. Marquez, J. Quijano and M. Gaulin<sup>5</sup> reported about a calibration technic to evaluate the power-law parameters of polymer melts using a torque rheometer with „promising technique to characterize polymeric melts using torque-rheometer measuring head.“ PVC was one of the investigated polymers. M. Bousmina, A. Ait-Kadi, and J. B. Faisant<sup>6</sup> reported about the determination of shear rate and viscosity based on torque rheometer data but not about PVC. In 2004 A. Mousa<sup>7</sup> published his studies on rheological behavior of thermoplastic elastomer derived from PVC and NBR by using torque rheometry. He reported that „the relationship obtained from the Brabender Plasticorder can be stated as:

$$M = C \cdot S^a \quad (12)$$

Where M is the torque, S is the rpm and C and a are constants. The above equation resembles the power law behaviour<sup>1, 8, 9</sup> which is given as:

$$\tau = K \cdot (\dot{\gamma})^n \quad (13)$$

where  $\tau$  is shear stress; K, constant;  $\dot{\gamma}$ , shear rate and n, non-Newtonian flow index.“ They calculated the Flow activation energy  $E_a$ .



## 2. Dryblend compositions

The dryblend compositions (Table 1) were mixed by Akdeniz Chemson Austria in Arnoldstein. Details about used raw materials, mixer and mixing conditions were not disclosed.

Table 1 Dryblend compositions

Dryblend =>	1	2	3	4	5	6	7	8	9	10
S-PVC (k = 55-57)	100									
S-PVC (k = 65-68)		100		100	100	100	100	100	100	100
S-PVC (k = 71 or higher)			100							
CaCarbonate, uncoated	10	10	10	20	10	10	10	10	10	10
Ca/Zn pipe stabiliser	2.5-3.0									
Calcium stearate					0.5					
Paraloid K 125 or similar						0.5				
Montanwax E							0.5			
GMS (90%)								0.5		
PE wax									0.5	
Hydrogenated castor oil										0.5

## 3. Equipments

The main investigations were made at Brabender GmbH & Co. KG in Duisburg, Germany by using the Plasticorder at 60 g dryblend, 180°C chamber temperature and at 45 rpm with software version 4.9.11. The extrusion was done with a counter-rotating twin screw extruder CTSE-V (Brabender, screw 404, die 2.0.2.10 cm<sup>3</sup>) with a slot capillary die and the software version 4.9.9. The extruder setup is shown in Figure 1. The density of all investigated dryblends were assumed to be 1.3 g/mL. Each dryblend was extruded at 15, 30, 40 and 60 rpm for about 20 to 25 min each rpm.

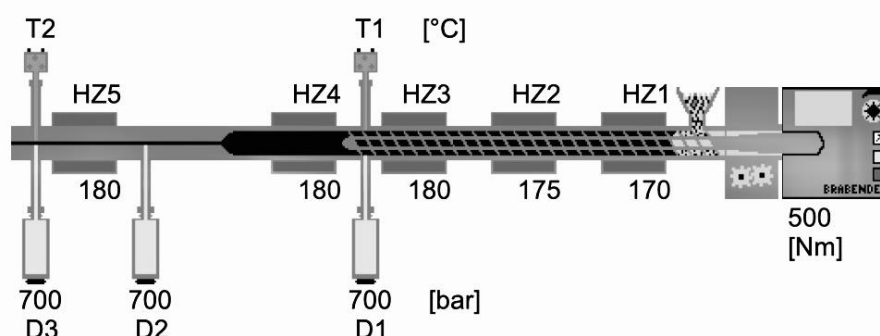


Figure 1 Extruder setup (HZ = heating zone, D1 to D3 = pressure transducer up to 700 bar, T1 and T2 = temperature sensor in °C, drive with 500 Nm maximum torque)



## 4. Results and discussion

### 4.1 Mathematical treatment of the torque rheometer data

Figure 2 shows a typical rheometer graph of dryblend 2 showing the dependency of torque and temperature on testing time inclusive the information about loading peak, minimum, inflection point maximum and end torque. There is a sudden drop at 8 to 9 minutes in each graph. This is related to the removal of the plunger closing the chamber.

However, it is also possible to extract the digital data from the plasticorder; Table 2 with the time in seconds, the experimental torque in Nm, the band width of experimental torque in Nm, the stock temperature transfer vom °C to Kelvin, the by Equation 9 calculated torque in Nm (beginning from maximum) and the difference in experimental and calculated torque. We calculated a flow activation energy  $E_a$  of 45.471 kJ/mol and  $M_0$  of 0.000269 Nm.

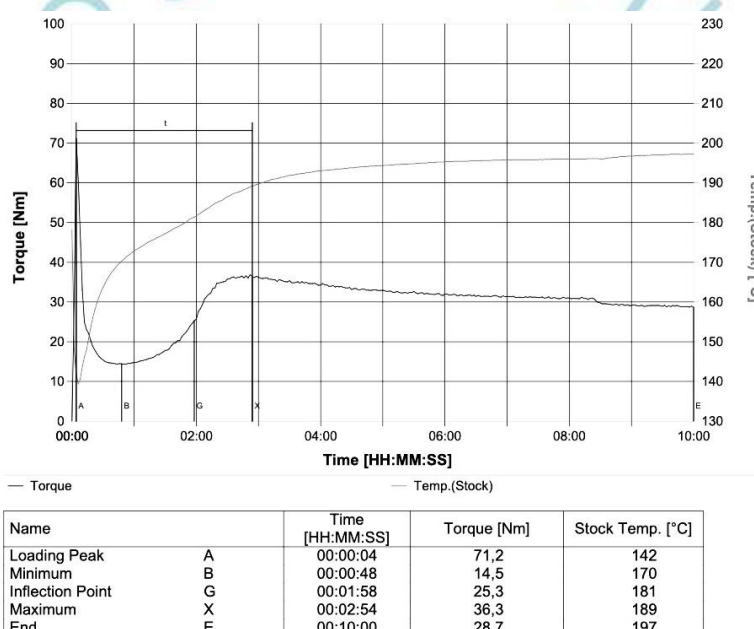


Figure 2 Torque rheometer graph of dryblend 2 as example; dependency of torque and temperature on testing time

In Figure 3 the overlay of the graph in Figure 2 (blue line), the experimental (green line) and calculated torque (red line) from Table 2 are plotted. It shows that there are minor differences. The experimental band width is in a range of 1.49 to 3.41 Nm beginning from the maximum torque while the difference of experimental and calculated torque is in a range of -0.21 to 1.26 Nm. We consider our simulation of the torque graph inside the range of the experimental error of the method.

Table 2 Digital data of Figure 2 until 8 minutes with the time in seconds, the experimental torque in Nm, the band width of experimental torque in Nm, the stock temperature transfer vom °C to Kelvin, the by Equation 6 calculated torque in Nm (beginning from maximum) and the difference in experimental and calculated torque (as typical example)





Time/s	Experimental torque/Nm	Bandwidth/Nm	Stock temperature/K	Calculated shear stressM/Nm at 197°C	(Exp. torque - shear stress)/Nm
0	0,0	0,01	451,3		
2	29,0	58,12	421,7		
4	71,2	21,78	415,0		
6	60,4	14,68	412,6		
8	47,1	19,52	413,8		
10	33,1	13,44	416,9		
12	24,9	3,86	419,4		
14	23,0	0,79	421,1		
16	22,1	2,01	424,0		
18	20,3	1,72	426,8		
20	18,9	1,25	429,1		
22	18,0	1,12	431,1		
24	17,0	0,80	432,9		
26	16,4	1,10	434,4		
28	15,8	0,66	435,8		
30	15,4	0,66	436,9		
32	15,0	0,69	438,0		
34	14,9	0,34	438,9		
36	14,7	0,44	439,8		
38	14,6	0,46	440,6		
40	14,5	0,59	441,2		
42	14,4	0,79	441,9		
44	14,4	0,68	442,5		
46	14,5	0,67	443,0		
48	14,5	0,62	443,5		
50	14,4	0,64	443,9		
52	14,4	0,68	444,5		
54	14,5	0,93	444,9		



Time/s	Experimental torque/Nm	Bandwidth/Nm	Stock temperature/K	Calculated shear stressM/Nm at 197°C	(Exp. torque - shear stress)/Nm
56	14,5	0,83	445,2		
58	14,7	0,65	445,7		
60	14,8	0,76	446,0		
62	14,8	0,82	446,4		
64	14,9	1,08	446,7		
66	15,2	1,03	447,0		
68	15,2	1,08	447,3		
70	15,4	0,92	447,6		
72	15,5	1,07	448,0		
74	15,8	1,10	448,3		
76	15,8	1,30	448,6		
78	16,0	1,38	448,8		
80	16,3	1,62	449,0		
82	16,8	1,28	449,4		
84	16,8	1,84	449,6		
86	17,1	1,58	449,9		
88	17,4	2,25	450,1		
90	17,8	1,65	450,4		
92	17,9	2,40	450,7		
94	18,3	2,23	451,0		
96	19,0	2,22	451,3		
98	19,6	2,16	451,6		
100	19,7	2,99	451,9		
102	20,3	2,68	452,1		
104	20,3	2,41	452,4		
106	21,3	2,59	452,7		
108	21,9	3,89	453,0		
110	22,4	2,64	453,3		



Time/s	Experimental torque/Nm	Bandwidth/Nm	Stock temperature/K	Calculated shear stressM/Nm at 197°C	(Exp. torque - shear stress)/Nm
112	23,1	2,82	453,7		
114	23,9	3,37	454,1		
116	24,6	3,79	454,3		
118	25,3	2,86	454,6		
120	25,7	2,84	454,9		
122	27,6	3,80	455,2		
124	28,3	2,80	455,6		
126	29,4	3,48	455,9		
128	30,8	3,20	456,3		
130	31,4	3,02	456,6		
132	31,9	2,89	456,9		
134	32,3	4,29	457,3		
136	33,5	3,43	457,7		
138	33,5	3,59	458,0		
140	34,8	2,56	458,2		
142	34,8	2,71	458,5		
144	35,0	2,20	458,7		
146	35,1	2,43	459,0		
148	35,2	2,67	459,4		
150	35,8	2,46	459,7		
152	35,8	2,22	459,9		
154	36,2	1,91	460,2		
156	36,3	2,24	460,5		
158	36,0	2,51	460,6		
160	36,2	2,04	460,8		
162	36,3	2,36	461,0		
164	36,6	2,44	461,2		
166	36,1	2,17	461,5		





Time/s	Experimental torque/Nm	Bandwidth/Nm	Stock temperature/K	Calculated shear stressM/Nm at 197°C	(Exp. torque - shear stress)/Nm
168	36,6	1,62	461,7		
170	36,0	2,90	461,9		
172	36,9	2,52	462,2		
174	36,3	2,31	462,4		
176	36,2	2,15	462,5		
178	36,5	2,40	462,8	36,5	0,0
180	36,2	2,64	462,9	36,4	-0,2
182	36,0	2,56	463,1	36,2	-0,2
184	35,9	2,73	463,2	36,1	-0,2
186	36,0	2,77	463,4	35,9	0,1
188	36,1	3,41	463,6	35,7	0,4
190	35,7	2,50	463,7	35,6	0,1
192	35,8	2,74	464,0	35,4	0,4
194	35,6	3,38	464,1	35,3	0,3
196	35,6	2,18	464,2	35,2	0,4
198	35,2	3,15	464,3	35,1	0,1
200	35,6	2,19	464,4	35,0	0,6
202	35,5	2,71	464,6	34,8	0,6
204	35,3	2,94	464,6	34,8	0,4
206	35,1	3,21	464,8	34,7	0,4
208	35,1	2,95	464,9	34,6	0,5
210	35,4	3,19	465,1	34,4	1,0
212	34,9	2,85	465,1	34,4	0,5
214	34,8	2,72	465,2	34,3	0,5
216	34,9	2,95	465,3	34,2	0,7
218	35,1	2,78	465,4	34,1	1,0
220	34,7	3,33	465,5	34,1	0,7
222	35,1	2,65	465,6	34,0	1,2
224	34,8	2,49	465,6	34,0	0,8
226	35,0	2,46	465,7	33,9	1,1



Time/s	Experimental torque/Nm	Bandwidth/Nm	Stock temperature/K	Calculated shear stressM/Nm at 197°C	(Exp. torque - shear stress)/Nm
228	34,7	2,69	465,7	33,9	0,8
230	34,6	2,81	465,8	33,8	0,8
232	34,6	3,35	465,9	33,7	0,9
234	34,7	2,67	466,0	33,6	1,1
236	34,5	2,86	466,1	33,5	0,9
238	34,2	3,04	466,2	33,5	0,7
240	34,3	2,60	466,2	33,5	0,8
242	34,6	2,62	466,3	33,4	1,3
244	34,3	2,80	466,3	33,4	0,9
246	34,3	3,21	466,4	33,3	1,0
248	33,9	2,65	466,4	33,3	0,7
250	34,0	1,96	466,5	33,2	0,8
252	34,2	2,27	466,5	33,2	1,0
254	33,8	2,65	466,6	33,1	0,7
256	34,0	3,28	466,7	33,0	0,9
258	33,8	2,47	466,7	33,0	0,8
260	33,9	2,58	466,7	33,0	0,9
262	33,7	3,17	466,8	33,0	0,7
264	33,6	2,66	466,9	32,9	0,7
266	33,5	2,60	466,9	32,9	0,6
268	33,7	2,39	467,0	32,8	0,9
270	33,1	2,34	467,0	32,8	0,3
272	33,4	2,82	467,0	32,8	0,6
274	33,4	2,26	467,1	32,7	0,7
276	33,1	2,44	467,1	32,7	0,4
278	33,1	2,80	467,2	32,6	0,4
280	33,2	2,47	467,2	32,6	0,6
282	33,3	2,69	467,2	32,6	0,6
284	33,0	3,18	467,3	32,5	0,5
286	33,0	2,13	467,3	32,5	0,4



Time/s	Experimental torque/Nm	Bandwidth/Nm	Stock temperature/K	Calculated shear stressM/Nm at 197°C	(Exp. torque - shear stress)/Nm
288	32,9	2,49	467,4	32,5	0,4
290	33,0	2,57	467,4	32,5	0,5
292	33,1	2,33	467,4	32,5	0,6
294	33,0	3,01	467,5	32,4	0,6
296	32,9	2,67	467,5	32,4	0,5
298	32,9	2,47	467,5	32,4	0,5
300	33,0	2,71	467,5	32,4	0,6
302	32,8	2,03	467,6	32,3	0,5
304	32,7	2,39	467,6	32,3	0,4
306	32,8	2,53	467,6	32,3	0,5
308	32,7	2,89	467,7	32,2	0,5
310	32,4	2,42	467,7	32,2	0,2
312	32,5	2,41	467,8	32,1	0,3
314	32,7	2,13	467,8	32,1	0,5
316	32,4	2,48	467,8	32,1	0,2
318	32,3	2,32	467,9	32,1	0,2
320	32,3	2,35	467,9	32,1	0,3
322	32,4	2,47	467,9	32,1	0,3
324	32,2	2,59	467,9	32,1	0,1
326	32,4	2,62	468,0	32,0	0,4
328	32,4	2,75	468,0	32,0	0,4
330	32,7	2,03	468,0	32,0	0,7
332	32,3	2,31	468,1	31,9	0,4
334	32,1	2,42	468,1	31,9	0,2
336	32,3	2,51	468,2	31,8	0,4
338	32,4	2,23	468,2	31,8	0,6
340	32,0	2,47	468,2	31,8	0,2
342	32,2	2,47	468,2	31,8	0,3
344	32,1	2,62	468,3	31,7	0,3
346	32,0	2,42	468,3	31,7	0,3



Time/s	Experimental torque/Nm	Bandwidth/Nm	Stock temperature/K	Calculated shear stressM/Nm at 197°C	(Exp. torque - shear stress)/Nm
348	31,9	2,38	468,3	31,7	0,2
350	31,9	2,13	468,3	31,7	0,2
352	32,1	3,08	468,4	31,7	0,4
354	32,2	2,32	468,4	31,7	0,5
356	31,7	2,58	468,4	31,7	0,1
358	31,7	2,51	468,4	31,7	-0,0
360	32,0	2,62	468,5	31,6	0,4
362	32,0	2,47	468,5	31,6	0,4
364	31,8	2,48	468,5	31,6	0,2
366	31,8	2,42	468,5	31,6	0,2
368	31,9	2,17	468,6	31,5	0,4
370	31,9	2,15	468,6	31,5	0,4
372	31,6	2,12	468,6	31,5	0,0
374	31,7	2,41	468,6	31,5	0,2
376	31,9	2,71	468,6	31,5	0,3
378	31,6	2,21	468,6	31,5	0,1
380	31,6	2,47	468,6	31,5	0,1
382	31,7	2,73	468,6	31,5	0,2
384	31,8	2,72	468,7	31,4	0,4
386	31,5	2,17	468,7	31,4	0,1
388	31,8	2,48	468,7	31,4	0,3
390	31,4	2,10	468,7	31,4	-0,0
392	31,6	2,49	468,7	31,4	0,2
394	31,5	2,24	468,7	31,4	0,0
396	31,4	2,18	468,8	31,4	0,1
398	31,4	2,57	468,8	31,4	0,1
400	31,4	2,50	468,8	31,4	0,1
402	31,5	2,50	468,8	31,4	0,1
404	31,4	2,13	468,8	31,4	0,0
406	31,5	2,28	468,9	31,3	0,2



Time/s	Experimental torque/Nm	Bandwidth/Nm	Stock temperature/K	Calculated shear stressM/Nm at 197°C	(Exp. torque - shear stress)/Nm
408	31,7	2,33	468,9	31,3	0,4
410	31,6	2,20	468,9	31,3	0,3
412	31,3	2,28	468,9	31,3	0,0
414	31,2	2,44	468,9	31,3	-0,1
416	31,6	2,42	469,0	31,2	0,4
418	31,3	2,38	468,9	31,3	0,1
420	31,4	2,24	469,0	31,2	0,2
422	31,4	2,29	469,0	31,2	0,2
424	31,3	2,72	468,9	31,3	0,1
426	31,5	2,13	469,0	31,2	0,3
428	31,2	2,34	469,0	31,2	-0,0
430	31,2	2,75	469,0	31,2	-0,0
432	31,2	2,60	469,0	31,2	0,0
434	31,1	2,58	469,0	31,2	-0,1
436	31,2	2,40	469,0	31,2	-0,0
438	31,3	2,27	469,0	31,2	0,1
440	31,2	2,72	469,0	31,2	-0,0
442	31,3	2,23	469,0	31,2	0,1
444	31,2	2,46	469,0	31,2	0,0
446	31,2	2,46	469,0	31,2	0,0
448	31,2	2,32	469,0	31,2	0,0
450	31,1	2,13	469,0	31,2	-0,1
452	31,2	2,25	469,1	31,1	0,0
454	31,3	2,41	469,0	31,2	0,1
456	31,0	2,26	469,1	31,1	-0,1
458	31,1	2,51	469,1	31,1	-0,0
460	31,3	2,22	469,1	31,1	0,2
462	30,9	2,52	469,1	31,1	-0,2
464	31,0	2,33	469,2	31,0	-0,0
466	31,1	2,08	469,2	31,0	0,1





Time/s	Experimental torque/Nm	Bandwidth/Nm	Stock temperature/K	Calculated shear stressM/Nm at 197°C	(Exp. torque - shear stress)/Nm
468	30,9	2,41	469,2	31,0	-0,1
470	30,8	2,59	469,2	31,0	-0,2
472	30,9	2,15	469,2	31,0	-0,2
474	31,2	2,26	469,2	31,0	0,2
476	31,0	2,52	469,2	31,0	-0,1
478	31,0	2,38	469,2	31,0	0,0
480	31,0	2,52	469,2	31,0	0,0

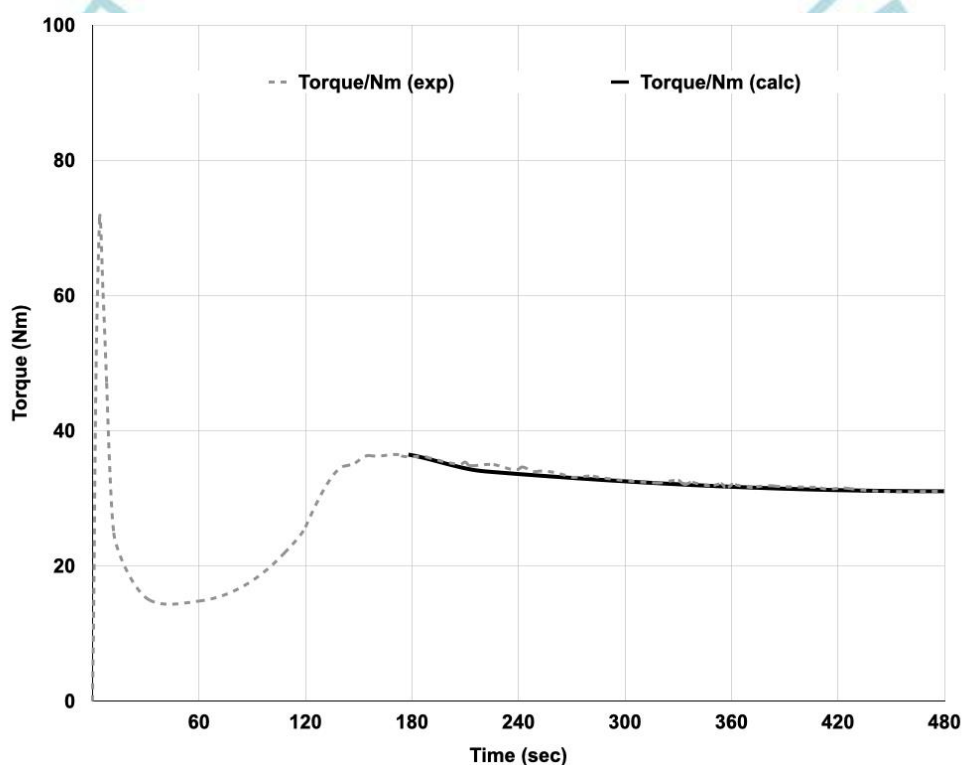


Figure 3 Overlay of the torque, the experimental torque (dotted, gray line) and calculated shear stress (black line) from Table 2

For the sake of completeness we also plotted the calculated vs the experimental torque (Figure 4) and found in tendency a more or less linear dependency with a regression coefficient of 0.9621. In tendency we found especially lower calculated values directly after the maximum. At the beginning we assumed that the actual temperature is during this time frame higher than the reported value. We tried simulations with different models but finally this cannot explain the comparably „low“ regression coefficient and non-linear shape in Figure 4. Today we assume something different:

During the time of measurement several chemical and physical reactions occurring during the treatment by heat and shear:



- HCl is released and reacting with the acid scavengers inside the stabiliser and increase the content of inorganic substances while the molecular weight of the degraded PVC is formed. Conjugated double bonds are formed which have a higher reactivity against radicals.
- Unstable chlorine is substituted by fatty acids and  $\beta$ -diketones
- The applied shear will result in scission of the PVC chain and form reactive polymeric radicals...
- De-agglomeration of filler and other inorganic additives
- Dispersion of filler and other inorganic additives

All these reactions might increase the viscosity of the polymer melt.

## 4.2 A kind for pre-trials

If we focus on the dryblends 1 to 3 the only variable will be the k value of PVC. There is an expected dependency on the viscosity number of the PVC resin on the k value<sup>3</sup>; Figure 5.

Viscosity number is the IUPAC term for reduced viscosity  $(\eta - \eta_0) / \eta_0 c$ ,

wherein is

$\eta$  the viscosity of the polymer solution

$\eta_0$  is the viscosity of the pure solvent

c is the concentration of the polymer solution (g) of solute per mL solution.

The rule of thumb: the higher the k value is the higher the viscosity number and finally the viscosity of the resin will be. If our hypothesis that it is possible to measure a kind of viscosity on torque rheometer is correct we'll find this back; Table 3 in which we calculated the flow activation energy  $E_a$  and the intrinsic torque  $M_0$ . Both for the flow activation energy  $E_a$  and the intrinsic torque  $M_0$  we did not any correlation or tendency. However, based on these values we calculated the apparent shear stress  $\tau/k$  at 197°C. We've chosen 197°C because it is ~480 Kelvin and corresponds with the melt temperature in extrusion of pipes and profiles.

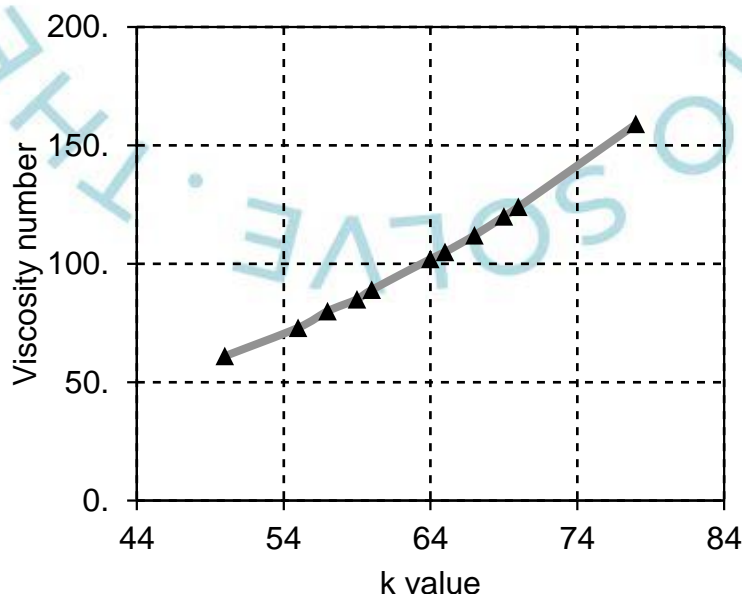


Figure 4 Calculated shear stress  $\tau/k$  at 197°C vs the experimental torque on torque rheometer



Table 3 Results on Brabender's plasticorder regarding dryblends 1 - 4 (2.5-3.0 phr Ca/Zn pipe stabiliser; 60 g sample, 45 rpm at 180°C)

Dryblend	1	2	3	4
PVC (k value)	55-57	65-68	71	65-68
phr CaCarbonate	10	10	10	20
	Plasticorder			
Max. torque/Nm	35,2	36,5	35,3	36,4
Temperature/K at maximum torque	444,6	462,8	467,6	461,4
Torque/Nm at 8 min	23,5	31,0	33,8	30,9
Temperature/K at 8 min	465,3	469,2	470,6	469,6
Flow activation energy/(J/mol)	33762	45471	26948	36030
M <sub>0</sub> /Nm	0,003804	0,000269	0,034436	0,003033
Regression coefficient	0,9777	0,9621	0,7257	0,9602
Apparent shear stress $\tau/k$ @ 197°C/Nm	21,5	30,4	34,0	30,6
	Single screw extruder			
$\tau$ /Pa at 15 rpm	55300	72800	85600	87500
$\tau$ /Pa at 30 rpm	74300	100000	108100	122300
$\tau$ /Pa at 40 rpm	85300	111500	113800	133900
$\tau$ /Pa at 60 rpm	109700	132200	132600	160200
$\eta$ /Pa·s at 15 rpm	1837	2435	3081	3148
$\eta$ /Pa·s at 30 rpm	1325	1854	2142	2446
$\eta$ /Pa·s at 40 rpm	1181	1608	1774	2060
$\eta$ /Pa·s at 60 rpm	1132	1332	1417	1266

In Figure 6 we plotted the apparent shear stress  $\tau/k$  at 197°C depending on the k value of PVC. In tendency we found a similar tendency like in Figure 5. Last but not least we found in Figure 7 that:

- The higher the k value of PVC is the higher the viscosity  $\eta$  will be at the same rpm and
- With increasing rpm the viscosity  $\eta$  will drop.

However, this is what was expected according to logic and experience. These 3 dryblends already indicate that our hypothesis regarding the measurement of viscosity with torque rheometer is not wrong; Figure 8. Dryblend 4 was considered as another supporting pretrial because the increasing content of Calcium carbonate shall result in an increasing viscosity. This was found in the extrusion results but not in the rheometer test. The explanation is very simple. Dryblend 4 has a higher density than the dryblends 1 to 3. Due



to this higher density the filling degree in the chamber of rheometer was lower. A lower filling degree will result in less shear, a later gelation and in a lower torque measurement.

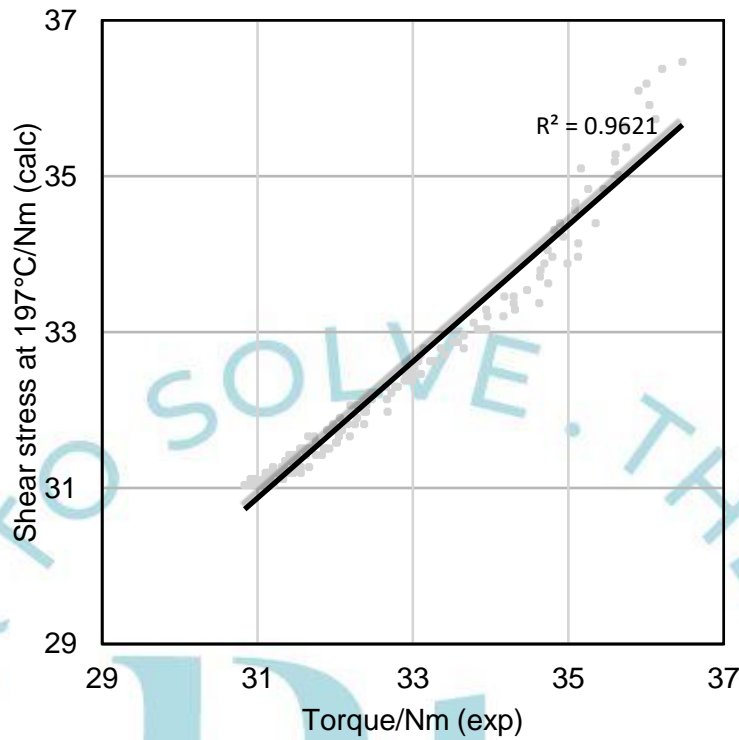


Figure 5 PVC Resin, k value vs Viscosity number (ISO 1628/2)<sup>10</sup>

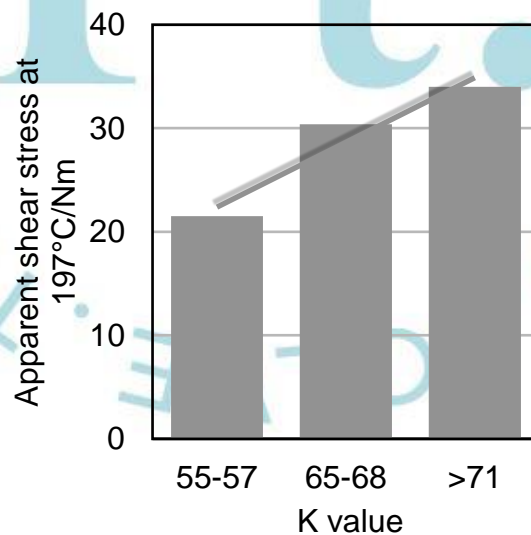


Figure 6 Dependency of apparent shear stress  $\tau/k$  at 197°C on the k value of PVC (data in table 3)

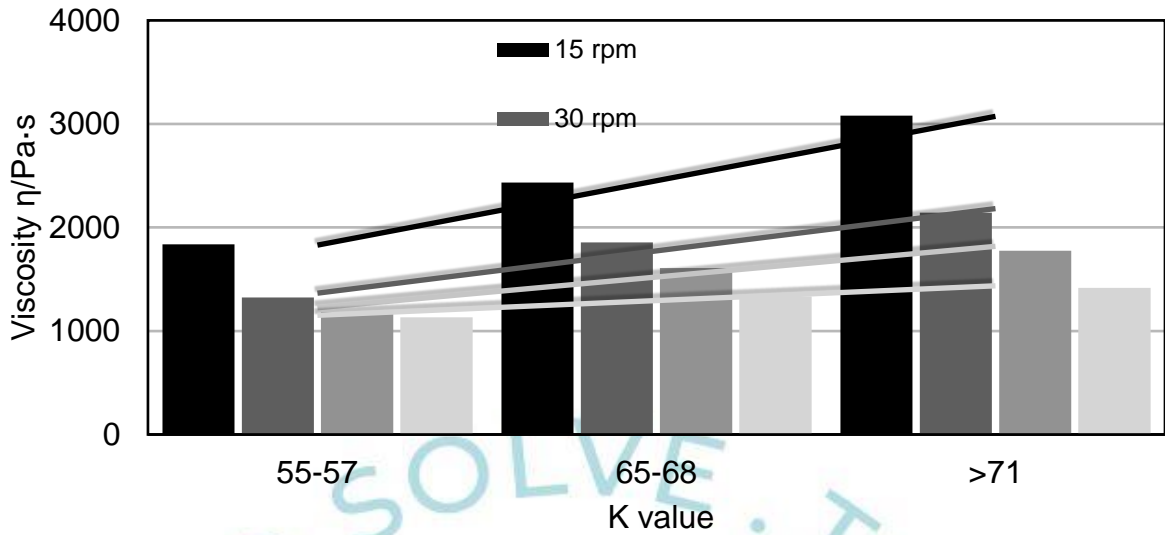


Figure 7 Dependency of viscosity  $\eta$  at different rpm on the k value of PVC (data in table 3)

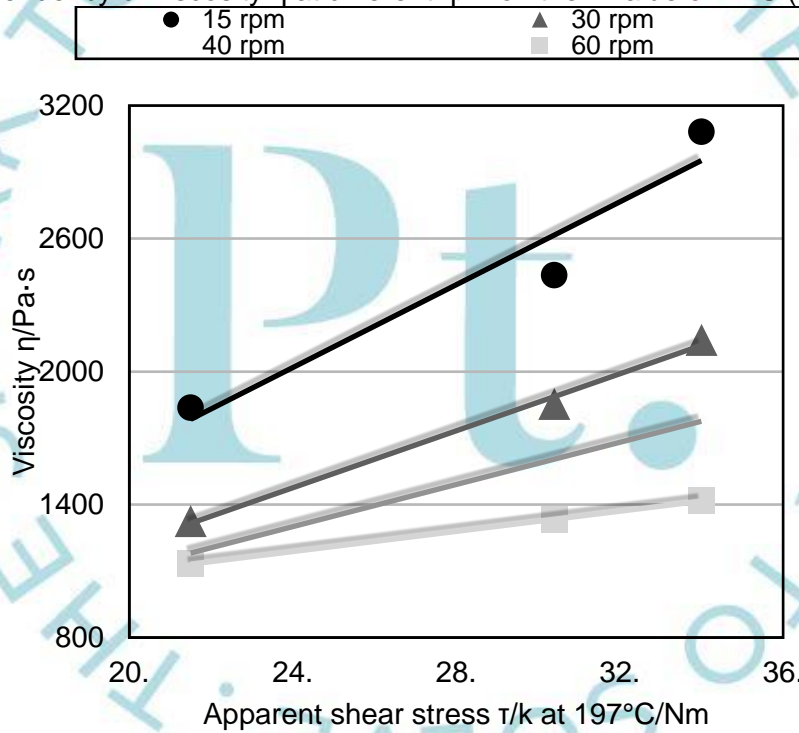


Figure 8 Dependency of viscosity  $\eta$  at different rpm on single screw extruder on apparent shear stress  $\tau/k$  at 197°C (data Table 3)





### 4.3 Main trials influences of additives

The dryblends 5 to 10 can be compared to dryblend 2. In all these dryblends the k value of the PVC and the amount of Calcium carbonate are constant. The main difference is the addition of 0.5 phr of an additive that influence the rheometer and extrusion results; Table 4. Unfortunately we could not receive a rheometer graph in the case of dryblend 9 with a PE wax. The dosage of PE wax too high. So, due to overlubrication no gelation of dryblend 9 was reached under the conditions of measurement.

Table 4 Results on Brabender's plasticorder regarding dryblends 2 and 5-10 (100 phr PVC [k = 65-68], 10 phr uncoated Calcium carbonate, 2.5-3.0 phr Ca/Zn pipe stabiliser; 60 g sample, 45 rpm at 180°C)

Dryblend	2	5	6	7	8	9	10
<b>0.5 phr of</b>	None	Calcium stearate	Acrylic processing aid, medium chain	Montan wax E	GMS (90%ic)	PE wax	HCO
	Plasticorder						
<b>Max. torque/Nm</b>	36,5	37,0	37,9	33,6	34,3	No signal	35,6
<b>Temperature/K at maximum torque</b>	462,8	462,9	460,8	462,7	461,9		462,0
<b>Torque/Nm at 8 min</b>	31,0	30,5	30,7	29,9	29,4		30,1
<b>Temperature/K at 8 min</b>	469,2	469,5	469,2	468,5	468,1		468,6
<b>Flow activation energy/(J/mol)</b>	45471	52686	45122	35833	44816		45835
<b>M<sub>0</sub>/Nm</b>	0,000269	0,000042	0,000291	0,003026	0,000293		0,000234
<b>Regression coefficient</b>	0,9621	0,9609	0,9587	0,9283	0,9749		0,9853
<b>Apparent shear stress <math>\tau/k</math> @ 197°C/Nm</b>	30,4	30,1	30,1	29,0	28,0	29,0	
	Single screw extruder						
<b><math>\tau</math>/Pa at 15 rpm</b>	72800	78900	74000	75600	64400		63400
<b><math>\tau</math>/Pa at 30 rpm</b>	100000	100400	98800	94500	86500		85100
<b><math>\tau</math>/Pa at 40 rpm</b>	111500	113900	112100	103600	102000		98300



Dryblend	2	5	6	7	8	9	10
$\tau/\text{Pa}$ at 60 rpm	132200	136900	132800	117200	127300		124800
$\eta/\text{Pa}\cdot\text{s}$ at 15 rpm	2435	2744	2506	2613	2226	2262	2183
$\eta/\text{Pa}\cdot\text{s}$ at 30 rpm	1854	2043	1848	1752	1559	1479	1583
$\eta/\text{Pa}\cdot\text{s}$ at 40 rpm	1608	1803	1621	1492	1418	1253	1430
$\eta/\text{Pa}\cdot\text{s}$ at 60 rpm	1332	1547	1357	1196	1282	894	1289

The graphs of calculated vs the experimental torque on torque rheometer show as a similar shape as in Figure 4: The regression coefficients (Table 4) are in a range of ~0.93 to ~0.99. The flow activation energies  $E_a$  in Table 3 and Table 4 are varying in a range of about 27 to 53 kJ/mol. (Any reaction with low activation energies like 10 kJ/mol is only slightly accelerated by increasing the temperature. In contrast, a high activation energy like 60 kJ/mol dramatically increases any reaction with increasing temperature. In the case of the

many molar/chemical the values of activation energies are in a range between 30 and 100 kJ/mol<sup>11</sup>.) We did not find any meaningful interpretation of the flow activation energy  $E_a$  and the intrinsic torque  $M_0$ . However, Figure 9 shows that there is a correlation between these.

In Figure 10 we plotted similarly to Figure 8 the relation between the viscosity  $\eta$  at different rpm on single screw extruder and the apparent shear stress  $\tau/k$  at 197°C based on the data 8n Table 4. The correlation is visible in tendency but it's difficult to impossible to discuss these effects related to the chemistry of the additives. The reason is very simple. The composition of the calcium-zinc stabilizer was not disclosed. There might be additives inside which can have a synergism with the additives in added to the dryblends 5 to 10. However, let's discuss the influence of the additives in comparison to dryblend 2 regarding our expectations in extrusion on a twin screw extruder in production. Calcium stearate (dryblend 4) does not effect the extrusion torque in our experience it only accelerates the fusion. We found a

- Slightly higher experimental maximum torque (+0.5 Nm) at the same mass temperature and
- Slightly lower calculated apparent shear stress  $\tau/k$  (-0.3 Nm).

Both findings correspond with our experience and our expectations. The acrylic processing aid with a medium molecular weight resp. a medium chain length behaves in our experience similarly to Calcium stearate regarding influence on fusion and extrusion torque. We found a:

- Slightly experimental maximum torque (+1.4 Nm) at the same mass temperature and
- Slightly lower calculated apparent shear stress  $\tau/k$  (-0.3 Nm).

Both findings confirm our expectation and experience. However, this is more obviously after mathematical treatment of the torque rheometer graph.

The other three additives belonging to the wide range of ester waxes:

- Montanester Wax E
- Glycerol monostearate (90%ic, GMS)
- Hydrogenated castor oil (HCO)

All of them are so called internal waxes for PVC and with some external functionality in the case of Wax E. We expected that Wax E would reduce the viscosity  $\eta$  resp. the apparent shear stress  $\tau/k$  more than GMO and much more than HCO. However, this was not found in tendency. Only speculations about reasons are possible.

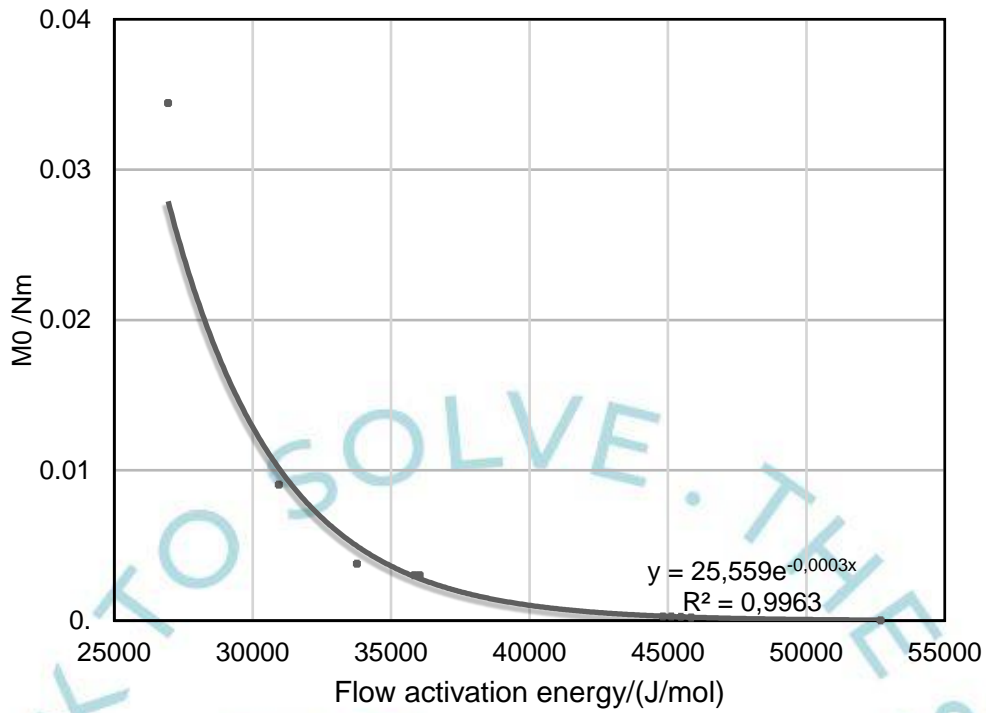


Figure 9 Dependency of intrinsic shear stress  $M_0$  on the flow activation energy  $E_a$

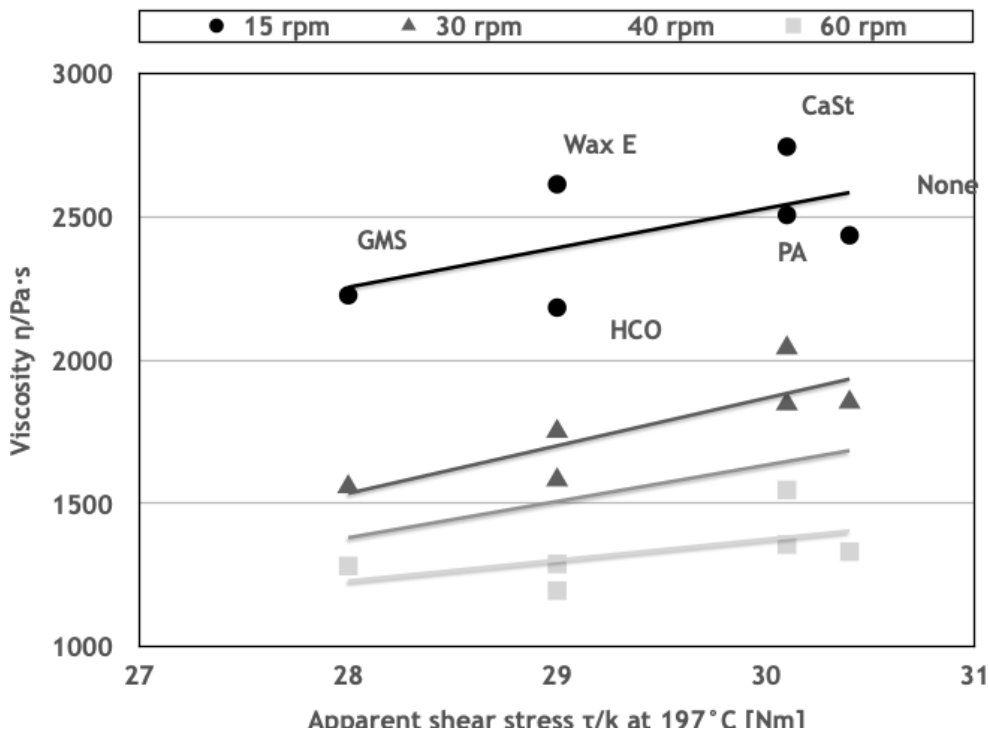


Figure 10 Dependency of viscosity  $\eta$  at different rpm on single screw extruder on apparent shear stress  $\tau/k$  at 197°C (data Table 4)



## 4.4 Reproducibility of the rheometer measurements and the calculations

Platinum Industries Pvt Ltd is a PVC well know stabiliser producer in the Indian PVC market, located in Mumbai. They repeated several times on different days with freshly mixed dryblend of the same composition the rheometer measurement under constant conditions; Table 5.

The gelation time has an average of 163 seconds and a standard deviation of 28 seconds which about 17% of average. This corresponds with the experience of the authors. While the experimental maximum torque has an average of 21.3 Nm (standard deviation: 1.5 Nm which is 6.9% of average) at 196.2°C in average (standard deviation: 0.9 degree) the calculated apparent shear stress  $\tau/k$  at 197°C is 20.9 Nm with a standard deviation of 1.1 Nm.

Table 5 Results on torque rheometer (not disclosed) regarding dryblends (100 phr PVC [k = 65-68], 10 phr uncoated Calcium carbonate, 0.2 phr lubricants, 2.5 phr pipe stabiliser; 68 g sample, 60 rpm at 180°C)

Serial number	Gelation time/s	Maximum torque/Nm	Temperature/°C at maximum torque	End torque/Nm (5 min)	Temperature/°C at end torque	M <sub>0</sub> /Nm	Flow activation energy/(J/mol)	Apparent shear stress $\tau/k$ @ 197°C/Nm
1	176	20,0	195,7	18,5	199,3	0,000720	39886	19,4
2	172	18,6	197,5	17,8	200,2	0,008361	30162	18,8
3	178	20,3	197,3	18,3	200,1	0,000000	68575	20,5
4	135	22,0	195,9	19,2	201,0	0,000070	49361	21,4
5	178	19,9	197,2	18,6	200,4	0,000906	39099	20,0
6	156	22,3	196,1	19,7	200,6	0,000048	50922	21,8
7	159	22,7	195,1	20,1	200,1	0,000227	44828	21,7
8	208	21,8	195,5	20,3	198,6	0,000424	42274	21,1
9	141	22,4	195,0	19,6	200,6	0,000278	43973	21,3
10	122	23,2	195,3	19,9	201,3	0,000125	47258	22,2
11	119	23,2	195,3	19,7	201,6	0,000103	48001	22,2
12	215	19,3	196,7	18,4	198,7	0,000247	44015	19,2
13	158	21,4	196,9	19,3	200,5	0,000027	53112	21,3
14	168	21,7	197,2	19,7	200,5	0,000020	54277	21,8
15	173	21,1	196,0	19,1	200,1	0,000215	44840	20,6
16	208	21,8	195,5	20,5	198,6	0,000424	42274	21,1



Serial number	Gelation time/s	Maximum torque/Nm	Temperature/°C at maximum torque	End torque/Nm (5 min)	Temperature/°C at end torque	$M_0$ /Nm	Flow activation energy/(J/mol)	Apparent shear stress $\tau/k$ @ 197°C/Nm
17	168	21,3	194,4	20,8	198,1	1,033831	11762	20,9
<b>Average</b>	166,7	21,4	196,0	19,4	200,0	0,061531	44389	20,9
<b>Standard deviation</b>	27,8	1,3	0,9	0,8	1,0	0,250564	11652	1,0

Figure 11 shows a linear relationship between the experimental maximum torque and the calculated apparent shear stress  $\tau/k$  at 197°C. The differences in experimental values can have different explanations:

- The torque rheometer measurement is not an absolute method.
- Small differences during dryblend preparation (weighing of raw materials, bulk density of raw materials, time, temperature...)
- Small differences during the measurement (weighing, fluctuations in start temperature, slide differences in rpm and bulk density of dryblend)
- Small difference in temperature graph during measurement (see standard deviation of temperature at maximum torque in Table 5)

However, it shows that this calculation method reduces the standard deviation of the apparent shear stress which can be considered as a normalization of the maximum torque to the same temperature of 197°C.

Furthermore, we found a high fluctuation in the flow activation energy  $E_a$  and the intrinsic torque  $M_0$ .

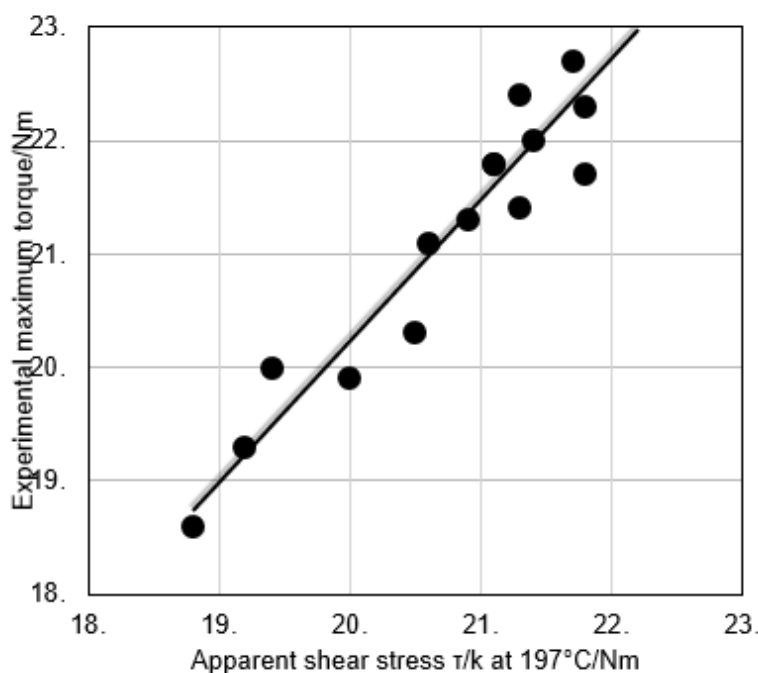


Figure 11 Relationship between experimental maximum torque and apparent shear stress  $\tau/k$  at 197°C (data Table 5)





## 5. Conclusion

One of our target was to simulate the rheometer graph by using Equation 6 which we reached in an acceptable good way. This allows to compare rheometer graphs at the same mass temperature (197°C in our case). Another benefit of this method is the reduction of standard deviation of the maximum torque at a normalized temperature. Another target was to proof that it is possible to measure shear stress resp. viscosities by using a torque rheometer. We found an excellent correlation between calculated shear stress  $\tau/k$  (rheometer) and the viscosity  $\eta$  (single screw extruder) in the case of PVC resins with different  $k$  values and an acceptable tendency of these during the measurement of 5 different additives. Last but not least we hoped to get reproducible results regarding the flow activation energy  $E_a$  and the intrinsic torque  $M_0$ .

Our next steps will be the repetition of the trials and the investigation of other additives.

## 6. Literature

<sup>1</sup> J. E. Goodrich, R. S. Porter; Polymer Engineering and Science, (01/1967) pp. 45-51

<sup>2</sup> C. V. Raman; „A theory of the viscosity of liquids“, Nature (London), 111 (1923) pp. 532-533

<sup>3</sup> E.N. da C. Andrade; "A Theory of the Viscosity of Liquids. - Part I.", London Edinb. Dub. Philos. Mag. J. Sci., 17(112), (1934) pp. 497–511

<sup>4</sup> Information provided by Brabender

<sup>5</sup> A. Marquez, J. Quijano, M. Gauli; Polymer Engineering and Science Vol. 36 No. 20 (10/1996) pp. 2556-2563

<sup>6</sup> M. Bousmina, A. Ait-Kadi, J. B. Faisant; J. Rheol. 43(2) (03-04/1999) pp. 415-433

<sup>7</sup> A. Mousa; Iranian Polymer Journal 13 (6) (2004) pp. 455-461

<sup>8</sup> L. I. Blyler, j. H. Dane; Polym. Eng. Sci., 7 (1967) pp. 178-181

<sup>9</sup> G. C. N. Lee, J. R. Purdon; Polym. Eng. Sci., 9 (1969) pp. 360-364

<sup>10</sup> <http://atozplastics.com/upload/literature/pvc.asp>; accessed on 26.06.2022

<sup>11</sup> G. Job, R. Ruffler: *Physikalische Chemie*, Vieweg+Teubner Verlag, Wiesbaden, 1. Auflage (2011), pp. 401–402